Available online at www.sciencedirect.com

SCIENCE DIRECT®

C. R. Physique 6 (2005) 133–137

COMPTES RENDUS PHYSIQUE

http://france.elsevier.com/direct/COMREN/

Physics/Mathematical physics, theoretical physics

A new reconstruction method in the Fourier domain for 3D positron emission tomography

Denis Mariano-Goulart [a], Jean-François Crouzet [b]

[a] *Department of nuclear medicine, Montpellier Medical University, 371, avenue du Doyen Giraud, 34295 Montpellier, France*
[b] *Department of mathematics, Montpellier Science University, place Eugène Bataillon, 34095 Montpellier, France*

Received 21 June 2004; accepted after revision 22 November 2004

Available online 28 December 2004

Presented by Maurice Goldman

Abstract

This article describes a new exact 3D reconstruction algorithm dedicated to cylindrical positron emission tomographs that does not require an estimation of missing projection data nor complex 3D interpolation procedures. This algorithm uses the 2D Fast Fourier Transform of non-transaxial projections to place suitable voxel values in the 3D FFT of the radioactive distribution. This leads to a direct fully 3D reconstruction algorithm with a limited amount of computation that requires only 1D interpolation procedures and benefits from redundant projection data to improve the signal to noise ratio in the radioactive distribution. ***To cite this article: D. Mariano-Goulart, J.-F. Crouzet, C. R. Physique 6 (2005).***

Résumé

Une nouvelle méthode de reconstruction 3D dans le domaine de Fourier en tomographie par émission de positons. Cet article décrit un nouvel algorithme exact de reconstruction 3D dédié aux tomographes par émission de positons cylindriques. Il ne nécessite pas l'estimation des données de projection manquantes ni d'interpolations délicates dans l'espace 3D. Il utilise la transformée de Fourier 2D de signaux construits à partir des projections obliques acquises pour calculer la transformée de Fourier 3D de la distribution de radioactivité à déterminer. On obtient ainsi un algorithme de reconstruction tridimensionnel rapide qui ne nécessite que des interpolations 1D et tire profit de la redondance des données de projection 3D pour autoriser un meilleur rapport signal sur bruit dans l'objet reconstruit. ***Pour citer cet article : D. Mariano-Goulart, J.-F. Crouzet, C. R. Physique 6 (2005).***

Keywords: Positron emission tomography; 3D reconstruction; Noise; Fourier transform

Mots-clés : Tomographie par émission de positons ; Reconstruction 3D ; Bruit ; Transformation de Fourier

E-mail addresses: d-mariano_goulart@chu-montpellier.fr (D. Mariano-Goulart), crouzet@math.univ-montp2.fr (J.-F. Crouzet).

1631-0705/$ – see front matter
doi:10.1016/j.crhy.2004.11.011

1. Introduction

The recent development of Positron Emission Tomography (PET) in functional imaging has made possible the use of 3D projection data in the tomographic reconstruction process. As collimators are no longer necessary when recording coincident events in a cylindrical PET scanner, this imaging technique provides measurements of line integrals of the radioactive tracer distribution (LOR) that are not restricted to lie within a plane perpendicular to the axis of the detector surface. Compared with the usual 2D reconstruction procedures used in Single Photon Computed Tomography, the LOR measured in a large solid angle surrounding the radioactive distribution are redundant so that the reconstruction algorithms that benefit from the maximum number of oblique projections are likely to produce a 3D reconstruction with a minimum amount of stochastic noise.

The generalization to 3D of usual 2D reconstruction algorithms based on the Fourier Slice Theorem (such as the filtered backprojection algorithm) requires measurements of projection data in a complete hemisphere. This condition is not satisfied for commercially available cylindrical PET scanners so that not all the projections that are necessary to reconstruct the radioactive distribution are recorded. As a consequence, the generalization to 3D of the usual backprojection algorithm [1–3] requires a first estimate of the unmeasured projection data [3–6]. This estimate is generally computed thanks to the forward projection of a first volumetric distribution reconstructed using 2D filtered backprojection (2D FBP) [6]. To date, the computational burden of this fully 3D reconstruction algorithm, as well as the complex 3D interpolation procedures required by the direct implementation of the Fourier slice theorem make these methods hardly compatible with clinical applications [7]. Moreover, the truncated projections are computed from a first noisy volumetric estimate of the radioactive distribution so that their statistic characteristics are decreased compared to the projections that are actually recorded.

A different approach uses approximations that sort the 3D projections into a 2D dataset containing one sinogram for each transaxial slice to be reconstructed. The resulting sinograms are processed using conventional 2D tomographic reconstruction algorithms. However, these rebinning algorithms are based on approximations that limit the resolution of the reconstruction or break down when the axial aperture of the scanner increases [7].

The purpose of this theoretical paper is to describe a new exact 3D reconstruction algorithm dedicated to cylindrical PET scanners that does not require estimation of missing projection data or complex 3D interpolation procedures. This algorithm uses the 2D Fast Fourier Transform (FFT) of non-transaxial projections to place suitable voxel values in the 3D FFT of the radioactive distribution. This leads to a direct fully 3D reconstruction algorithm that requires only a limited amount of computation.

2. Posing the problem

Let us consider a cylindrical PET scanner of radius R and length H, with its horizontal axis along the x_3-axis (Fig. 1). Any plane orthogonal to the axial direction x_3 will be called a transaxial plane. Any point a on the detector surface can be defined by $a = (R\cos\theta_a, R\sin\theta_a, z_a)$, with $0 \leqslant \theta_a < 2\pi$ and $0 \leqslant z_a \leqslant H$. A couple of photons emerging from an elementary volume of activity corresponds to a certain LOR intersecting the detector at two opposite points a and a', and having an unit directional vector $\omega = (\cos\theta\sin\varphi, \sin\theta\sin\varphi, \cos\varphi)$, with the Euler's angles ranging $0 \leqslant \theta < 2\pi$ and $0 \leqslant \varphi \leqslant \pi$.

For whole body measurements, the height H of the cylinder is much smaller than the height L of distribution of activity in the patient. This is the reason why it is necessary to operate a sequence of translations of the PET scanner along the x_3-axis. Let us denote λH (typically with $\lambda = 1/4$) the length of the superposition of two consecutive translations of the PET detector, γ and γ' the distances covered by the translations of the PET scanner before and after the radioactive distribution. The effective field of view of the PET scanner will be the cylindrical volume $V = \{(x_1, x_2, x_3) \in \mathbb{R}^3,\ x_1^2 + x_2^2 \leqslant R^2,\ 0 \leqslant x_3 \leqslant \gamma + L + \gamma'\}$ (Fig. 2).

If one considers a couple of opposite points (a, a') and all the vectors ω of the unit sphere, one can make a first natural restriction on the angle φ: $0 \leqslant \varphi \leqslant \frac{\pi}{2}$. Let us consider the direction ω of a given coincidence ray coming from any elementary distribution of radioactivity located in the cylindrical volume V. The invariance by translations of the 3D projection data states that for all point a on the detector surface, the line integral corresponding to (a, ω) is actually recorded. As shown in Fig. 2,

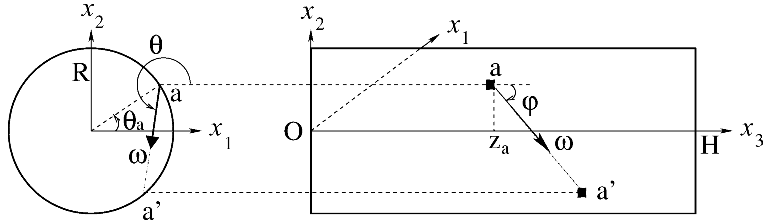

Fig. 1. Transverse and longitudinal projection views of a cylindrical PET scanner.

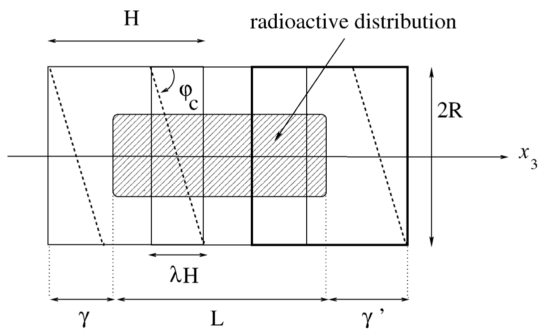

Fig. 2. Three translations of a cylindrical PET scanner illustrating the definitions of φ_c, γ and γ'.

this condition leads to $\tan\varphi \geqslant (2R)/(\lambda H)$. We will demonstrate in the next paragraph that invariance by translations of the 3D projection data as well as a last condition stating that $\varphi \neq \frac{\pi}{2}$ are necessary and sufficient to construct the algorithm proposed in this article. This leads to the final conditions:

$$\arctan\left(\frac{2R}{\lambda H}\right) = \varphi_c \leqslant \varphi < \frac{\pi}{2}, \tag{1}$$

with $\gamma > \lambda H$ and $\gamma' > \lambda H$.

Remark 1. In the case of focal acquisitions, no translation of the cylindrical PET is necessary and one gets the value $\varphi_c = \max(\arctan(\frac{2R}{\gamma}), \arctan(\frac{2R}{\gamma'}))$.

3. The Fourier-based 3D reconstruction method

Let $f \in L^2(\mathbb{R}^3)$ with support in $\{(x_1, x_2, x_3) \in \mathbb{R}^3,\ x_1^2 + x_2^2 < R^2,\ \gamma < x_3 < L + \gamma\}$ be the finite energy signal corresponding to the distribution of radioactivity. The positions of the detectors a which record signals from the distribution of radioactivity correspond to $z_a \in [0, L + \gamma]$ along the x_3-axis. Consider the line integral $P_f(a, \omega)$ measured by the pair of detectors (a, a') in the direction ω. For all $\theta_a \in [0, 2\pi[$, $z_a \in [0, L + \gamma]$, $\theta \in [0, 2\pi[$, $\varphi \in [\varphi_c, \frac{\pi}{2}[$:

$$P_f(a, \omega) = \int_{\mathbb{R}} f(a + t\omega)\,\mathrm{d}t = \int_{\mathbb{R}} f(R\cos\theta_a + t\cos\theta\sin\varphi, R\sin\theta_a + t\sin\theta\sin\varphi, z_a + t\cos\varphi)\,\mathrm{d}t. \tag{2}$$

The change of variable $u = z_a + t\cos\varphi$, with $\cos\varphi > 0$, leads to

$$P_f(a, \omega) = \int_{\mathbb{R}} f\left(R\cos\theta_a + \frac{u - z_a}{\cos\varphi}\cos\theta\sin\varphi, R\sin\theta_a + \frac{u - z_a}{\cos\varphi}\sin\theta\sin\varphi, u\right)\frac{\mathrm{d}u}{\cos\varphi}. \tag{3}$$

If one denotes

$$(X_1, X_2) = (R\cos\theta_a - z_a\tan\varphi\cos\theta,\ R\sin\theta_a - z_a\tan\varphi\sin\theta), \tag{4}$$

Eq. (3) becomes $P_f(a, \omega) = \frac{1}{\cos\varphi}\int_\gamma^{L+\gamma} f(X_1 + u\tan\varphi\cos\theta, X_2 + u\tan\varphi\sin\theta, u)\,\mathrm{d}u$. Let us define, $\forall (x_1, x_2) \in \mathbb{R}^2$, $\forall \theta \in [0, 2\pi[$, $\forall \varphi \in [\varphi_c, \frac{\pi}{2}[$

$$p_{\theta,\varphi}(x_1, x_2) = \frac{1}{\cos\varphi}\int_\gamma^{L+\gamma} f(x_1 + u\tan\varphi\cos\theta, x_2 + u\tan\varphi\sin\theta, u)\,\mathrm{d}u. \tag{5}$$

This leads to

$$P_f(a, \omega) = p_{\theta,\varphi}(X_1, X_2). \tag{6}$$

We now look for a necessary and sufficient condition under which the set of projections recorded by the cylindrical PET scanner makes possible the computation of $p_{\theta,\varphi}$ over its whole support.

Let us define the line segment $L_{\theta,\varphi} = \{(-z_a\tan\varphi\cos\theta, -z_a\tan\varphi\sin\theta),\ 0 \leqslant z_a \leqslant L + \gamma\}$, for any given values for θ and φ (Fig. 3). A LOR can be recorded only if $\theta - \theta_a \in]\frac{\pi}{2}, 3\frac{\pi}{2}[$. Thus for $\theta_a \in]\theta + \frac{\pi}{2},\ \theta + 3\frac{\pi}{2}[$, and for $z_a \in [0, L + \gamma]$,

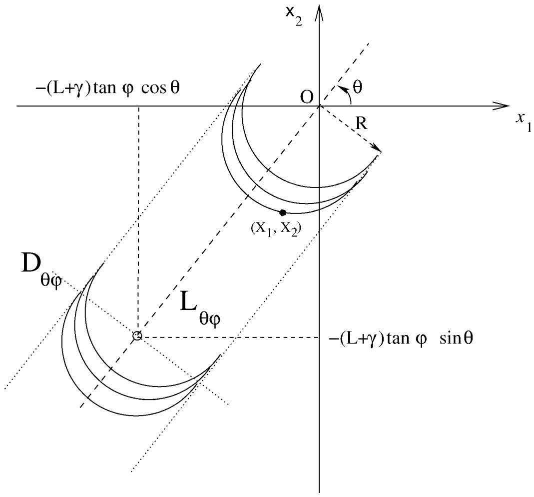

Fig. 3. The domain $D_{\theta,\varphi}$.

(X_1, X_2) describes a reunion of semi-circles with radius R, centered on $L_{\theta,\varphi}$. If one assumes that $\tan\varphi \geqslant (2R)/(\lambda H)$, the length $(L+\gamma)\tan\varphi$ of $L_{\theta,\varphi}$ is greater than the diameter $2R$ of the semi-circles. Then the points (X_1, X_2) fill the whole domain $D_{\theta,\varphi} = \{x = (x_1, x_2) \in \mathbb{R}^2,\ \mathrm{d}(x, L_{\theta,\varphi}) \leqslant R\}$, where $\mathrm{d}(x, L_{\theta,\varphi})$ is the Euclidian distance from a point x to the set $L_{\theta,\varphi}$.

Consider any point $x = (x_1, x_2) \notin D_{\theta,\varphi}$ verifying $\mathrm{d}(x, L_{\theta,\varphi}) > R$.

Thus, $\forall u \in [0, L+\gamma]$, $(x_1 + u\tan\varphi\cos\theta)^2 + (x_2 + u\tan\varphi\sin\theta)^2 > R^2$. As the support of the distribution of radioactivity f is included in a cylinder of radius R, whose horizontal axis is the x_3-axis, the term in the integral of Eq. (5) is zero.

Then $(x_1, x_2) \notin D_{\theta,\varphi} \Rightarrow p_{\theta,\varphi}(x_1, x_2) = 0$. Thus the values of $p_{\theta,\varphi}$ are known on a domain $D_{\theta,\varphi}$ that contains the support of $p_{\theta,\varphi}$.

Reciprocally, let us assume that $\tan\varphi < (2R)/(\lambda H)$, that is $\lambda H < 2R/(\tan\varphi)$. For any pair of detectors a and a', say for any ray (a, ω), one easily shows that $z_{a'} - z_a = -(2R\cos(\theta - \theta_a))/\tan\varphi \leqslant (2R)/(\tan\varphi)$. As a consequence, there exists an infinite set of couples of detectors a and a' for which $\lambda H < z_{a'} - z_a \leqslant 2R/\tan\varphi$ whose LOR $P_f(a, \omega)$ cannot be recorded by the PET (Fig. 1). As X_1 and X_2 in Eq. (4) are continuous with respect to the angular variable θ_a and to the longitudinal variable z_a, there exists subsets of $D_{\theta,\varphi}$ of non-zero measure in $\mathbb{R}^2$ that are not reached by any (X_1, X_2).

This completes the proof that $\varphi \geqslant \varphi_c = \arctan((2R)/(\lambda H))$ is necessary and sufficient to calculate $p_{\theta,\varphi}$ over its whole support from the projection data measured in a cylindrical PET scanner. Thus the condition (1) makes possible the computation of its 2D Fourier transform $\widehat{p_{\theta,\varphi}}$.

Let us denote $\tilde{f}$ the Fourier transform of f along the two first variables. The inversion formula of the Fourier transform in L^2 and the definition (5) leads to

$$p_{\theta,\varphi}(X_1, X_2) = \frac{1}{\cos\varphi} \int_{\gamma}^{L+\gamma} \left(\iint_{\mathbb{R}^2} \tilde{f}(\xi_1, \xi_2, u) \mathrm{e}^{2\mathrm{i}\pi((X_1 + u\tan\varphi\cos\theta)\xi_1 + (X_2 + u\tan\varphi\sin\theta)\xi_2)} \,\mathrm{d}\xi_1\,\mathrm{d}\xi_2 \right) \mathrm{d}u. \tag{7}$$

Using a truncation of the integrals on $\mathbb{R}^2$, Fubini's theorem and the definition of the Fourier transform in L^2, one can show that Eq. (7) leads to

$$p_{\theta,\varphi}(X_1, X_2) = \frac{1}{\cos\varphi} \iint_{\mathbb{R}^2} \left(\int_{\gamma}^{L+\gamma} \tilde{f}(\xi_1, \xi_2, u) \mathrm{e}^{2\mathrm{i}\pi(u\tan\varphi(\xi_1\cos\theta + \xi_2\sin\theta))} \,\mathrm{d}u \right) \mathrm{e}^{2\mathrm{i}\pi(X_1\xi_1 + X_2\xi_2)} \,\mathrm{d}\xi_1\,\mathrm{d}\xi_2 \tag{8}$$

$$= \frac{1}{\cos\varphi} \iint_{\mathbb{R}^2} \left(\int_{-\infty}^{+\infty} \tilde{f}(\xi_1, \xi_2, u) \mathrm{e}^{-2\mathrm{i}\pi(-u\tan\varphi(\xi_1\cos\theta + \xi_2\sin\theta))} \,\mathrm{d}u \right) \mathrm{e}^{2\mathrm{i}\pi(X_1\xi_1 + X_2\xi_2)} \,\mathrm{d}\xi_1\,\mathrm{d}\xi_2 \tag{9}$$

$$= \frac{1}{\cos\varphi} \iint_{\mathbb{R}^2} \hat{f}\big(\xi_1, \xi_2, -\tan\varphi(\xi_1\cos\theta + \xi_2\sin\theta)\big)\, \mathrm{e}^{2\mathrm{i}\pi(X_1\xi_1 + X_2\xi_2)} \,\mathrm{d}\xi_1\,\mathrm{d}\xi_2. \tag{10}$$

Let us call $\widehat{p_{\theta,\varphi}}$ the 2D Fourier transform in L^2 of the function $p_{\theta,\varphi}$. As we have shown that $p_{\theta,\varphi}(X_1, X_2)$ provides a complete knowledge of $p_{\theta,\varphi}$, the uniqueness of the inverse Fourier transform leads to

$$\forall(\xi_1,\xi_2)\in\mathbb{R}^2,\quad \widehat{p_{\theta,\varphi}}(\xi_1,\xi_2)=\frac{1}{\cos\varphi}\hat{f}\big(\xi_1,\xi_2,-\tan\varphi(\xi_1\cos\theta+\xi_2\sin\theta)\big). \tag{11}$$

Last, let us show that for all real ξ_3 and $(\xi_1,\xi_2)\neq(0,0)$, there exists a couple (θ,φ), with $0\leqslant\theta<2\pi$ and $\varphi_c\leqslant\varphi<\frac{\pi}{2}$, verifying $\xi_3=-\tan\varphi(\xi_1\cos\theta+\xi_2\sin\theta)$.

Since ξ_3 describes the interval $[-\tan\varphi\sqrt{\xi_1^2+\xi_2^2},\ \tan\varphi\sqrt{\xi_1^2+\xi_2^2}]$ and $\lim_{\varphi\to\frac{\pi}{2}}\tan\varphi=+\infty$, then ξ_3 describes $\mathbb{R}$. Therefore (ξ_1,ξ_2,ξ_3) describes $\mathbb{R}^3$ except the two half-lines defined by $\{(\xi_1,\xi_2,\xi_3)\in\mathbb{R}^3,\ |\xi_3|>0,\ \xi_1=\xi_2=0\}$.

As a consequence, the Fourier transform $\hat{f}$ is known almost everywhere so that its inverse Fourier transform can be computed.

This completes the proof that f can be determined from the projection data $P_f(a,\omega)$ by means of Eqs. (6) and (11). The practical conditions for performing the various FFTs are not discussed in the present article. They will be described in a forthcoming publication.

4. Conclusion

In this theoretical article, we proved that a volumetric distribution of radioactivity can be reconstructed using the 2D Fast Fourier Transform of data derived from non-transaxial projections and 1D interpolation procedures. As for a given $(\xi_1,\xi_2)\in\mathbb{R}^{2*}$, the function $(\theta,\varphi)\to-\tan\varphi(\xi_1\cos\theta+\xi_2\sin\theta)$ is surjective but not injective on $\mathbb{R}$, Eq. (11) allows redundant evaluation of $\hat{f}$ almost everywhere in the 3D space. As the projections acquired in an actual PET scanner are noisy, this redundancy can be averaged to improve the signal to noise ratio in the evaluation of $\hat{f}$. This will provide a full 3D reconstruction algorithm in which the use of oblique projections will allow a better control of stochastic noise compared with the results achieved with usual 2D reconstruction algorithms.

Moreover, the use of only one 3D FFT in the reconstruction of the whole distribution ensures that this algorithm will be able to provide reconstructions more rapidly than other usual 3D reconstruction algorithms.

References

[1] S.S. Orlov, Theory of three dimensional reconstruction. I. Conditions for a complete set of projections, Sov. Phys. Crystal. 20 (1976) 312–314.

[2] S.S. Orlov, Theory of three dimensional reconstruction. II. The recovery operato, Sov. Phys. Crystal. 20 (1976) 429–433.

[3] J.G. Colsher, Fully three-dimensional PET, Phys. Med. Biol. 25 (1980) 103–115.

[4] J.G. Rogers, R. Harrop, P.E. Kinahan, The theory of three-dimensional image reconstruction for PET, IEEE T. Med. Imaging 6 (1987) 239–243.

[5] M. Defrise, D.W. Townsend, R. Clack, Image reconstruction from truncated two-dimensional projections, Inverse Probl. 11 (1995) 287–313.

[6] P.E. Kinahan, J.G. Rogers, Analytic 3D image reconstruction using all detected events, IEEE T. Nucl. Sci. 36 (1989) 964–968.

[7] M. Defrise, P.E. Kinahan, W. Townsend, C. Michel, M. Sibomana, D.F. Newport, Exact and approximate rebinning algorithms for 3D PET data, IEEE T. Med. Imaging 16 (1997) 145–158.